ISET Journal of Earthquake Technology, Paper No. 395, Vol. 36, No. 2-4, June-Dec. 1999, pp.121-137

COMBINED CONTROL STRATEGY: BASE ISOLATION AND TUNED MASS DAMPING

Bruno Palazzo and Luigi Petti
Dipartimento di Ingegneria Civile,
Università di Salerno, Italy

ABSTRACT

A new control strategy which combines tuned mass damping (TMD) with base isolation (BI) concept is discussed in this paper by summarizing the working properties of the dual control strategy. To visualize the relationships between dynamic variables and subsystems, block-diagram illustrations are used which provide a mechanical view of this control strategy. It is shown that the BI technique applies an open-loop control law and that TMD uses a closed-loop control law. Seismic performances of combined systems are summarized showing numerical response tests of models subject to some recorded seismic excitations in linear and non-linear range and to stationary Gaussian random processes. Control effectiveness of TMD in reducing seismic vibrations of base isolated systems is compared with that produced by adding damping in the isolation layer.

KEYWORDS: Base Isolation, Tuned Mass Damper, Combined Passive Control Strategy

INTRODUCTION

The tuned mass damper (TMD) can be considered to be a new version of the dynamic vibration absorber invented by Frham in the United States in 1909 (Frham 1909). As is known, the auxiliary tuned mass dampers system (Figure 1) is capable of reducing the main system response near the tuned frequency (Den Hartog, 1956; Ormondroy et al., 1928) while the higher modes are marginally influenced (Chang et al., 1980).

During the last twenty years, TMD have been installed in a great number of tall buildings in many parts of the world, mainly in the U.S. and Japan, to reduce vibrations in main systems. The effectiveness of this system in reducing wind-excited structures is now well-established (Kitamura et al., 1988). The application of this methodology for the reduction of seismic vibrations of systems fixed at the base leads to uncertain results: a good performance with large response reduction in the case of excitations with strong components near the resonance was found by Villaverde in 1994 (Villaverde, 1994); in other cases, fixed-base structures under seismic excitations have generally shown little or even no effect since the different frequency contributions are not attenuated (Kaynia et al. 1981).

During the same period, research on base isolation (BI) system (Figure 2) has increased exponentially (Kelly, 1990; IASMIRT; 1991). A great number of buildings have also been constructed in this period using base isolation technique in many countries throughout the world. As is known, the effectiveness of BI depends on the low-pass filtering capacity of the frequency ranges where the earthquake energy is strongest and closest to the fundamental natural vibration frequency of the superstructure. The filtering effect mainly influences the superstructure inter-storey drifts concentrating large deformations into the isolation bearings. Therefore, the central problem of the BI strategy is that, under certain excitations, systems can undergo excessive displacements at the base.

Observing that well-isolated system responses are dominated by the first-modal contribution and that TMD are able to reduce the fundamental vibration mode, a new idea of combining both properties into a unique system has been proposed and investigated by Palazzo et al. (1994), (see Figure 3). The objective is to control the system response by only reducing the fundamental modal contribution which is dominant in such systems.

The positive behavior is due to the appropriate combination of three fundamental properties of the original systems:

1. the reduction in the ground motion transmission to the superstructure;
2. the vibration mode modification due to the BI;

3. the first vibration mode reduction by means of the TMD to this frequency.

The main working principle is summarized below along with the seismic performance of BI and TMD strategy, considering mechanical aspects, showing linear response to recorded earthquakes and to random excitations. Non-linear response due to the non-linear behavior of isolators is examined later.

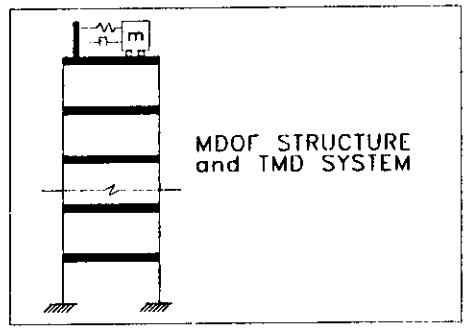

Fig. 1 Fixed base structure and TMD

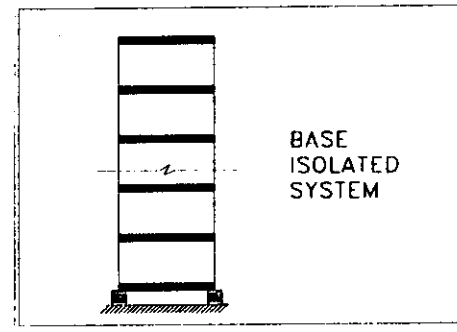

Fig. 2 Base isolated system

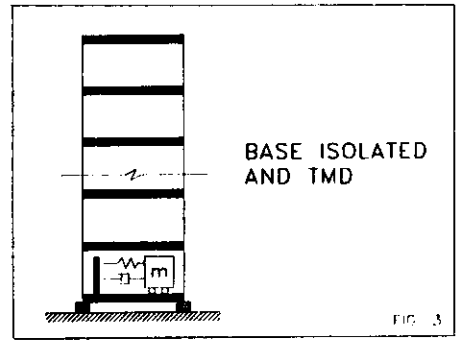

Fig. 3 Base isolation and TMD

ASPECTS OF STRUCTURAL VIBRATION PASSIVE CONTROL BY USING BLOCK DIAGRAM DESCRIPTION

The relationships between cause (input) and effect (output) of any system may be represented by a block diagram. This is the graphic representation of functional I/O (input/output) of system elements providing a visual description of the interactions of the various elements according to their mathematical relationships (Figure 4).

Fig. 4 Block diagram

In order to obtain I/O relations (transfer operators) of different blocks in a linear system, it is convenient to operate with Laplace operator which converts the linear differential equations of motion into algebraic equations. In this case, the relationships between input and output are described by transfer functions H(s).

As is known, control systems can be classified into two categories: systems with open loop control laws and systems with closed loop control laws.

An open loop control system is one in which the control action is independent from the output, as shown in Figure 5. Consequently, the controller does not know what is happening to the response of the structure. As shown, the control law which is represented by G(s), is a way of filtering the input signal to the primary system described by H(s).

In a closed loop control system, the control action depends in some way on the output which is therefore called feedback because it comes from a sequence between cause and effect (Figure 6). As seen, by this control law, a portion of the output signal transformed by the operator G(s) is fed back to the main system described by H(s).

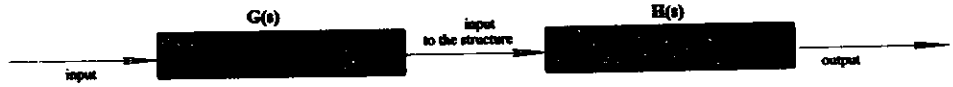

Fig. 5 Open loop control scheme

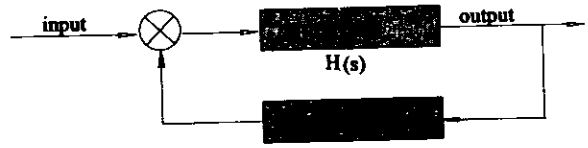

Fig. 6 Feedback control scheme

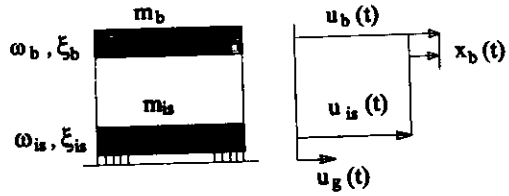

Fig. 7 Base isolated system model

1. Base Isolation Strategy

Let us consider the two-degree of freedom base isolated system model shown in Figure 7. It is constituted by the superstructure frequency ω_b and damping factor ξ_b if fixed at the base, and by the isolation system frequency . ω_{is} and damping ξ_{is}, if rigidly oscillating on isolators.

The motion equation is given by:

$$\begin{cases} \ddot{x}_b + 2\xi_b\omega_b\dot{x}_b + \omega_b^2 x_b = -\ddot{u}_{is} \\ \ddot{u}_{is} + 2\xi_{is}\omega_{is}\dot{u}_{is} + \omega_{is}^2 u_{is} = 2\xi_{is}\omega_{is}\dot{u}_g + \omega_{is}^2 u_g - \chi\ddot{x}_b \end{cases} \tag{1}$$

where $\chi = \dfrac{m_b}{m_b + m_{is}}$ represents the mass ratio. By applying the Laplace transform to (1) and reordering, the following transfer relationships are obtained (Palazzo et al., 1997):

$$\begin{aligned} X_b &= \frac{H_b(s)G(s)}{1 - B(s)H_b(s)} U_{is}(s) \\ U_{is} &= \frac{G(s)}{1 - B(s)H_b(s)} U_g(s) \end{aligned} \tag{2}$$

where $B(s) = \dfrac{-s^2\chi}{s^2 + 2\xi_{is}\omega_{is}s + \omega_{is}^2}$; $H_b(s) = \dfrac{-s^2}{s^2 + 2\xi_b\omega_b s + \omega_b^2}$; $G(s) = \dfrac{2\xi_{is}\omega_{is}s + \omega_{is}^2}{s^2 + 2\xi_{is}\omega_{is}s + \omega_{is}^2}$

In Equation (2), the term $B(s)H_b(s)$ represents the interaction between the superstructure and the isolated base.

It is possible to numerically show that when the coupling degree $\Omega = \omega_{is}/\omega_b$ becomes small, as in the case of optimal isolation, the interaction term provides an insignificant contribution to the overall system response in the frequency range of interest. In those cases, Equations (2) reduce to:

$$\begin{aligned} X_b &= H_b(s)G(s)U_{is} \\ U_{is} &= G(s)U_g \end{aligned} \tag{3}$$

To show the insignificant role performed by the interaction term $B(s)H_b(s)$, the magnitude and the phase of the base displacement transfer function related to the ground motion, computed by the exact form (last of Equation (2), dotted line in Figures 8-9) and by the approximate one (last of Equation (3), solid line in Figures 8-9) are plotted in Figures 8-9.

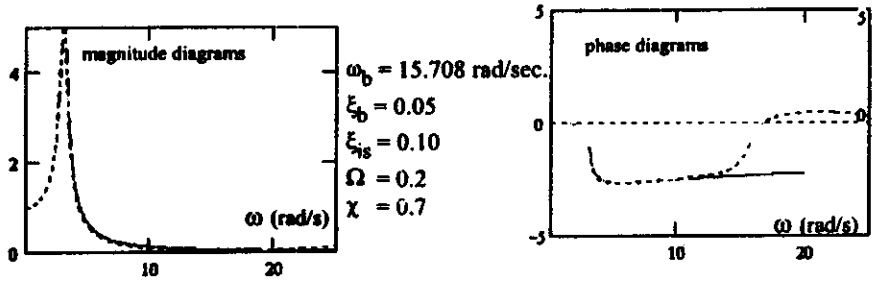

Figs. 8,9 Exact (dot line) and approximated (solid line) transfer functions of magnitude and phase respectively

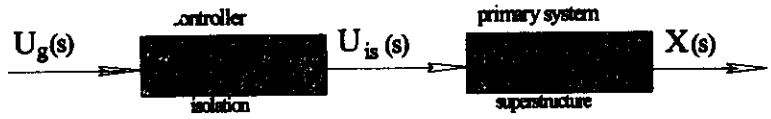

Fig. 10 Simplified block-diagram representing base isolation

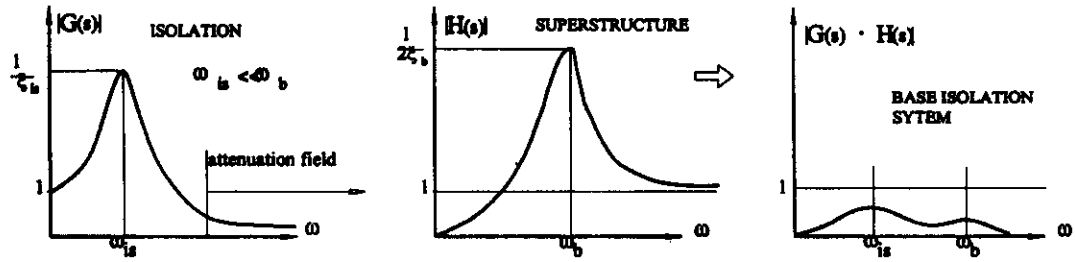

Fig. 11 BIS functional principle

The magnitude diagrams of transfer function $G(s)$ show good agreement between the exact values and the approximate ones. The phase diagrams show significant differences only in the high frequency range where the magnitude diagram presents very low amplifications. Differences between the exact formulation and the approximate one decrease with the decreasing of coupling degree Ω and mass ratio χ.

The first in Equation (3) shows that the seismic base isolation strategy acts as the open loop scheme shown in Figure 10 if the interaction produced by the superstructure shift on the isolation plane is neglected. Therefore, from a physical viewpoint, in a fixed base system, the base excitation is directly applied to the structure while in a base isolated system, the base excitation is filtered by the isolation level which acts as a controller regulating the excitation transmission to the superstructure. The qualitative behavior of $G(s)$ and $H(s)$ reported in Figure 11 shows that the efficiency of base isolation depends on

the ratio of superstructure fundamental frequency ω_b to the overall system frequency firmly oscillating on isolators ω_{is}, defined as isolation degree (Palazzo, 1991):

$$I_d = \omega_b / \omega_{is}$$

The same figure shows how it is possible to favorably regulate the relationship between the excitation and the superstructure response by choosing a soil-isolation transfer function $G(s)$ in order to attenuate the superstructure frequency response, choosing $\omega_{is} << \omega_b$.

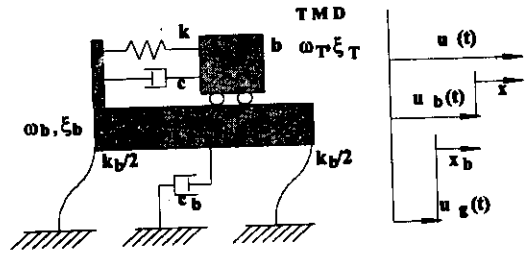

Fig. 12 SDOF and TMD model

2. Mass Damping Strategy

The objective in adding a TMD satellite system is to bring the main structure resonant peak of the amplitude down to its lowest possible value. In this case, the excitation of a controlled system activates the TMD, generally placed on roofs, capturing energy from the main system on which it applies a phase opposition inertial feedback.

The motion equation of two degrees of freedom linear model, shown in Figure 12 is given by:

$$\begin{aligned} &\ddot{u} + 2\xi_T \omega_T \dot{u} + 2\omega_T^2 u = 2\xi_T \omega_T \dot{u}_b + \omega_T^2 u_b \\ &\ddot{u} + 2\xi_b \omega_b \dot{u}_b + \omega_T^2 u_b = 2\xi_b \omega_b \dot{u}_g + \omega_T^2 u_b - \mu \ddot{u} \end{aligned} \tag{4}$$

where ξ_T and ω_T, respectively, represent the damping factor and the natural frequency of the satellite system (TMD), while ξ_b and ω_b are the corresponding quantities of the main system; the mass ratio is expressed by parameter $\mu = m/m_b$.

By applying the Laplace transform and reorganizing Equation (4), we obtain:

$$\begin{aligned} &U = G(s) U_b \\ &U_b = H_b(s) U_g + H_b(s) \frac{-s^2 \mu}{2\xi_b \omega_b s + \omega_b^2} U = H_b(s) U_g + H_b(s) \alpha(s) U \end{aligned} \tag{5}$$

which show the I/O links of controlled system.

With $\alpha(s) = \dfrac{-s^2 \mu}{2\xi_b \omega_b s + \omega_b^2}$, the transfer operator $H_c(s)$ of the overall system is then given by (Palazzo et al., 1997):

$$U_b = \frac{H_b(s)}{1 + H_b(s) \alpha(s) G(s)} U_g = H_c(s) U_g \tag{6}$$

Equation (6) corresponds to the scheme given in Figure 13. As seen in Figure 13 and in the sequence of diagrams in Figure 14, by appropriately choosing $G_T(s) = G(s)\alpha(s)$, we can obtain a resonance reduction of the main system. It can be shown that when this control system is applied to a multi-degree of freedom system, it allows a reduction of the amplification only in a narrow band of frequencies, generally centered on the fundamental frequency. Therefore, the efficiency of TMD for the reduction of vibrations originating from seismic activity of a higher degree of freedom system is not significant considering that the frequency content of excitation is extended to a wider frequency spectrum.

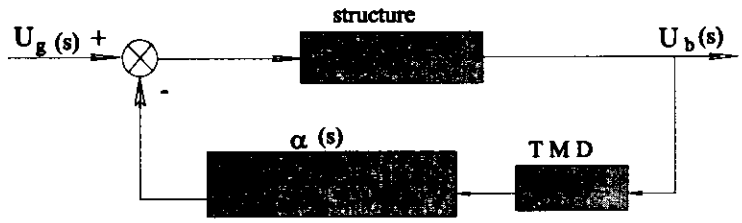

Fig. 13 Mass damping block diagram

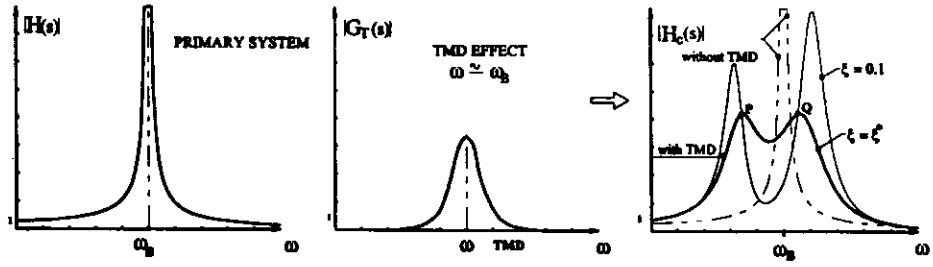

Fig. 14 TMD functional principle

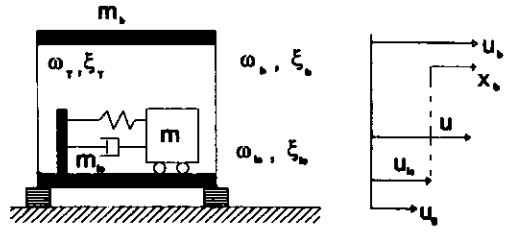

Fig. 15 Base isolated system provided with TMD

3. The Combined System: Base Isolation & Mass Damping

Let us consider the three degree of freedom model of the combined system BI & TMD shown in Figure 15.

Given ω_b and ξ_b, ω_{is} and ξ_{is}, ω_T and ξ_T the natural frequencies and the damping factors of the superstructure, isolation and TMD, respectively, the motion equations of the model can be written as:

$$\begin{aligned} &\ddot{u} + 2\xi_T\omega_T\dot{u} + 2\omega_T^2 u = 2\xi_T\omega_T\dot{u}_{IS} + \omega_T^2 u_{is} \\ &\ddot{x}_b + 2\xi_b\omega_b\dot{x}_b + \omega_b^2 x_b = -\ddot{u}_{is} \\ &\ddot{u}_{is} + 2\xi_{is}\omega_{is}\dot{u}_{is} + \omega_{is}^2 u_{is} = 2\xi_{is}\omega_{is}\dot{u}_g + \omega_{is}^2 u_g - m\ddot{u} - m\ddot{x}_b \end{aligned} \tag{7}$$

where μ and χ indicate the two mass ratios $\mu = \dfrac{m}{m_b + m_{is}}$ and $\chi = \dfrac{m_b}{m_b + m_{is}}$.

As in the previous cases, by operating the Laplace transforms and organizing, we obtain:

$$\begin{aligned} &U = G(s)U_{is} \\ &X_b = H_b(s)U_{is} \\ &U_{is} = G_{is}(s)U_{ig} + G_{is}(s)\frac{-s^2\mu}{2\xi_{is}\omega_{is}s + \omega_{is}}U + B(s)X_b \end{aligned} \tag{8}$$

Even in this case, regarding well-designed systems, we can show the insignificant influence of the interaction term $B(s)X_b$ in the last equation in Equation (8) which becomes (Palazzo et al., 1997):

$$U_{is} \cong G_{is}(s)U_{ig} + G_{is}(s)\alpha(s)U \quad \text{with} \quad \alpha = \frac{-s^2\mu}{2\xi_{is}\omega_{is}s + \omega_{is}}$$

and therefore we obtain:

$$X_b = \frac{G_{is}(s)}{1 + G_{is}(s)\alpha(s)G(s)} \cdot H_b(s) \cdot U_g \qquad (9)$$

This corresponds to the control scheme shown in Figure 16.

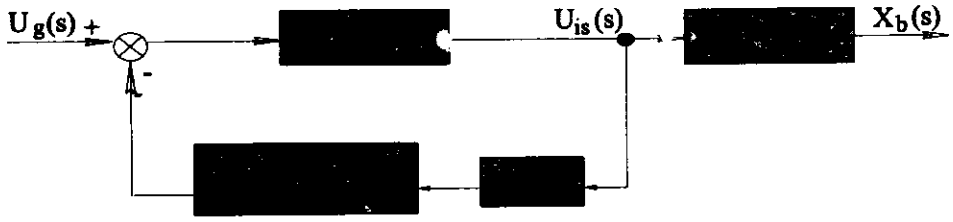

Fig. 16 Block diagram of the combined control system "Base Isolation + TMD"

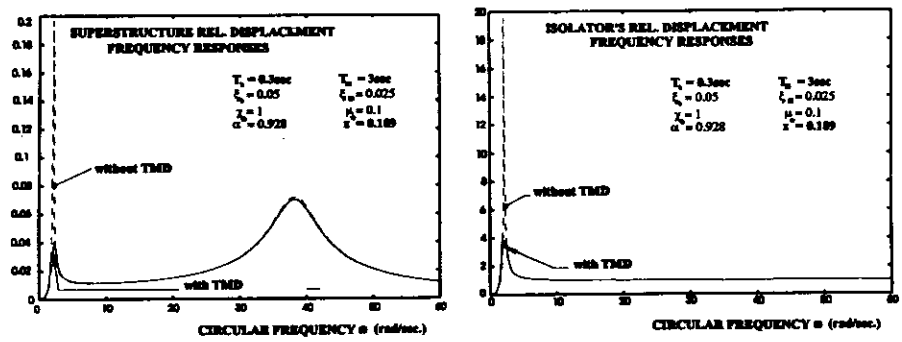

Fig. 17a TMD function principle (α^* optimal tuning ratio)

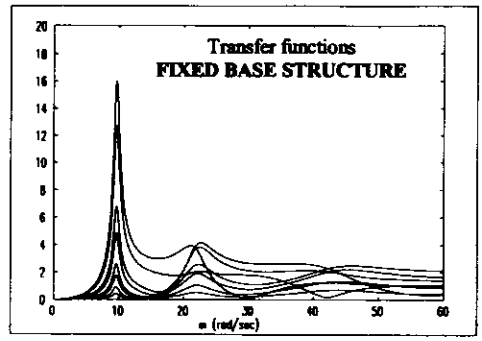

Fig 17b Fixed base 10-storey structure frequency response
($T_d = 0.2$ sec, $\xi_b = 0.05$, $\xi_{is} = 0.02$, $I_d = 3$)

As seen from transfer functions plotted in Figure 17(a), the effect of TMD, reduction of amplification in a narrow band, favorably combines with BI because, as is well known, the fundamental mode is strongly dominant in isolated systems. The reduction effects produced by the combination strategy are

stronger for the MDOF structures (Figure 17(b)). In fact, the favorable high frequency filtering, produced by the isolation allows to reduce the overall system response even if the TMD selective narrow frequency band suppressing is used (Figure 17(c)).

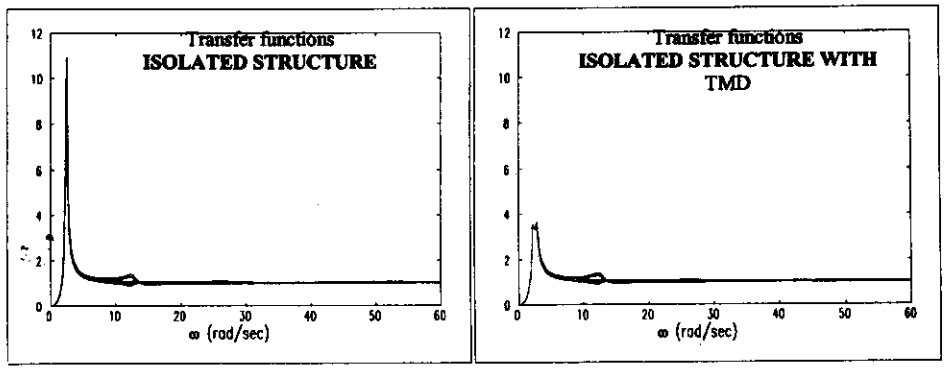

Fig. 17c Base isolated 10-storey structure frequency response with and without TMD ($T_d = 0.2$ sec, $\xi_b = 0.05$, $\xi_{is} = 0.02$, $I_d = 3$)

SEISMIC RESPONSE COMPARISON OF BASE ISOLATED SYSTEMS WITH AND WITHOUT TMD IN LINEAR RANGE

The elastic responses of BI model with and without TMD subjected to several excitations have been comparatively analyzed. The investigation was carried out by analyzing a multi degree-of-freedom system. TMD parameters have been chosen according to optimum parameters reported in the reference (Ioi et al., 1978), for systems subjected to seismic excitations.

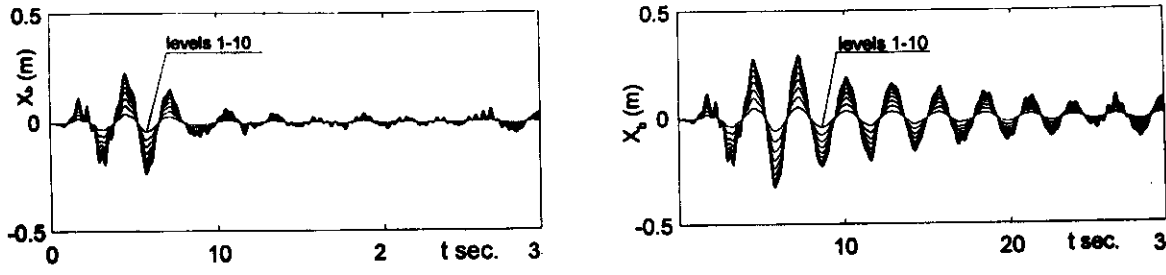

Figs. 18,19 10 story isolated building model - Superstructure story displacement time histories with and without TMD ($T_b = 0.67$ sec; $\xi_b = 0.02$, $\xi_{is} = 0.05$, $I_d = 4$ - EQ: El Centro, 1939)

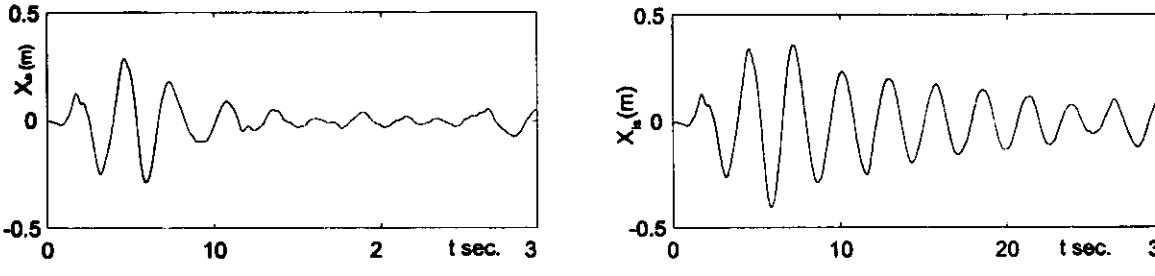

Figs. 20-21 10 story isolated building model - Base relative displacement time histories with and without TMD ($T_b = 0.67$ sec; $\xi_b = 0.02$, $\xi_{is} = 0.05$, $I_d = 4$ - EQ: El Centro, 1939)

The response comparisons with and without TMD are shown in Figures 18-21 subject to the El Centro earthquake N-S 1939. Figures 18-19 show the superstructure response with and without TMD. Figures 20-21 show the base response with and without TMD.

Results show that the use of TMD to control seismic vibrations of BI, significantly improve the general performance of the systems. Comparisons show significant reductions in relative base displacements due to the absorbers. The illustrated results indicate that the use of TMD has the advantage of absorbing the seismic energy without contaminating the high frequencies filtering effect of the isolation.

RESPONSE OF BASE ISOLATED AND TMD SYSTEMS TO RANDOM EXCITATIONS

The response in linear range of two degree of freedom base isolated systems controlled by TMD subject to a stationary Gaussian random process is discussed below.

The parametric study is focussed in showing the influence of the TMD and isolation parameters on the response of the doubly controlled system. The investigation is relevant in evaluating the root mean square (RMS) gain obtainable by adding a TMD to a base isolated system and in establishing the appropriate parameters of the isolation layer and those of the satellite mass damper.

In this analysis, the horizontal ground acceleration $a_g(t)$ is modeled as a stationary Gaussian filtered white noise random process with a zero mean and characterized by its Power Spectral Density (PSD), $S_{ag}(\omega)$. In particular, the PSD formulation proposed by Kanai (1957) and Tajimi (1960), and later modified by Clough et al. (1975) by applying a low frequency filter is used as a spectrum model. Soil is considered in the analysis by assuming the following in the spectrum model: $\omega_g = 31.4$ rad/sec; $\xi_g = 0.55$. For all cases, the characteristics of Clough-Penzien modification low-band frequency filter are assumed as: $\omega_1 = 1$; $\xi_1 = 0.7$.

Figures 22-25 show the ratios of the RMS response quantities concerning BI with TMD compared to the corresponding ones relative to base isolated systems without TMD. In particular, the quantities considered are the relative displacements. Figures show that doubly controlled systems generally have a 50% response reduction compared to base isolated systems in a wide range of parameters.

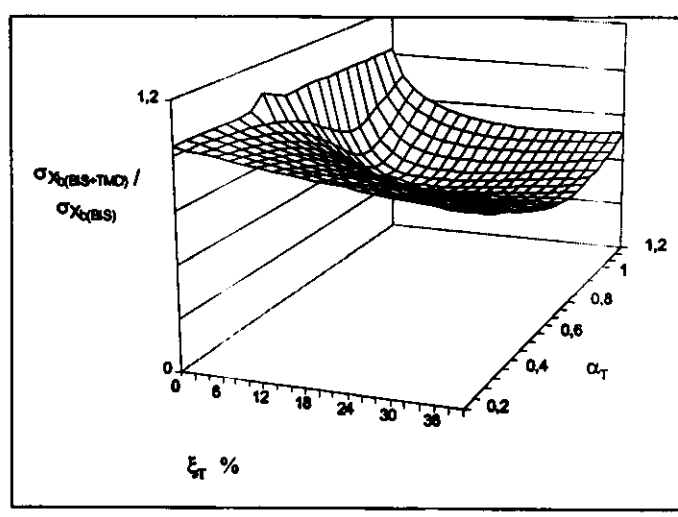

Fig. 22 Superstructure relative displacement RMS ratio
($T_b = 0.5$ sec; $\xi_b = 0.02$, $\xi_{is} = 0.05$, $I_d = 5$; $\mu = 0.10$)

The influence of the TMD tuning parameters $\alpha_T = \omega_T/\omega_{is}$ and ξ_T on the system behavior is illustrated in Figures 22-23. From the plotted diagrams, it can be noted that the optimum tuning

parameters agree with the Ioi-Ikeda (Ioi et al., 1978) ones. Moreover, the response sensitivity of the new system is slightly influenced by small tuning parameter variations.

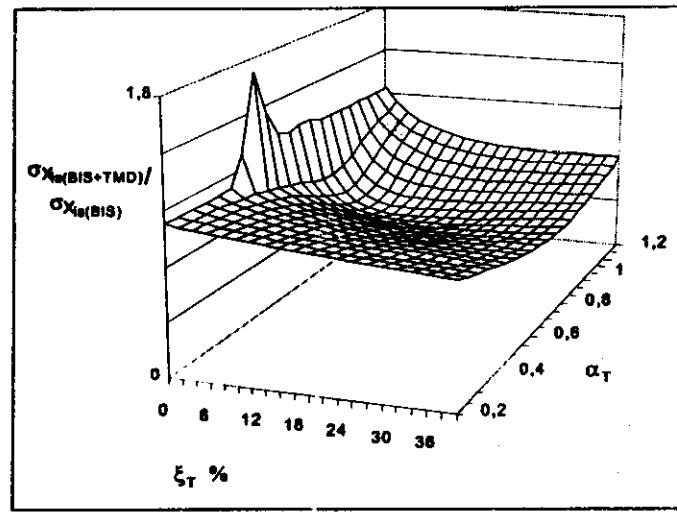

Fig. 23 Isolators relative displacement RMS ratio
(T_b= 0.5 sec; ξ_b = 0.02, ξ_{is} = 0.05, I_d = 5; μ = 0.10)

Results presented in Figure 24 show the influence of the original period T_b and the isolating degree I_d, as previously defined. The isolation degree, I_d, does not affect the TMD effectiveness.

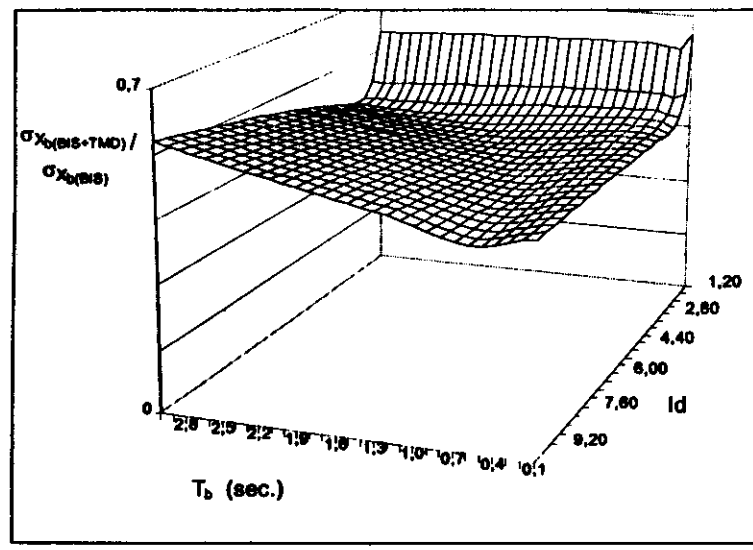

Fig. 24 Superstructure relative displacement RMS ratio
(ξ_b = 0.02, ξ_{is} = 0.05, μ = 0.10)

The influence of both the mass ratio, μ, and the original period, T_b, is illustrated in Figure 25. The benefits produced by the TMD strongly increase for values of $\mu = 0.05 - 0.10$ and much less so for greater values.

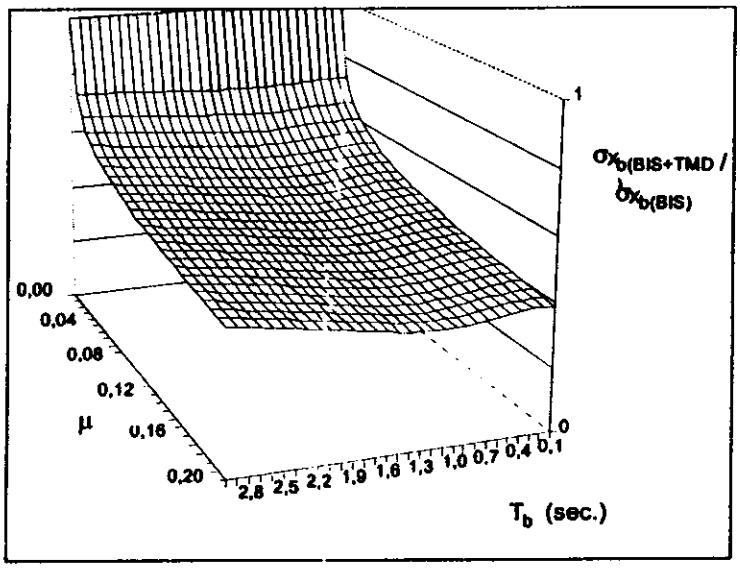

Fig. 25 Superstructure relative displacement RMS ratio
($\xi_b = 0.02$, $\xi_{is} = 0.05$, $\mu = 0.10$)

In all the examined cases, the superstructure RMS response remains lower than the corresponding one of base isolated systems. The superstructure RMS acceleration response ratios are identical to the displacement ones as shown in Palazzo et.al. (1997).

SEISMIC RESPONSE OF BASE ISOLATED SYSTEMS WITH AND WITHOUT TMD IN NON LINEAR RANGE

In this section, the effect of the combined TMD and BI strategy in the presence of isolators with a non-linear behavior is examined. In fact, in the case of non-linear behavior, the effectiveness of an auxiliary system (TMD) could diminish due to the loss of tuning with the fundamental variable frequency of the main system. This implies that there could be a dependency of the response reduction attained on the isolator hysteretic characteristics.

Considering the multi-degree of freedom isolated structure and the auxiliary mass (TMD), described by an equivalent linear model, and the non linear behavior of the isolators represented by the Bouc-Wen-Baber (BWB) model (Tajimi, 1960), the complete mathematical model may be written as follows:

$$\begin{aligned} \mathbf{I}\,\ddot{\mathbf{x}} + 2\xi\,\Omega\,\dot{\mathbf{x}} + \Omega\,\mathbf{x} &= -\mathbf{1}\ddot{u}_g - \mathbf{1}\ddot{x}_{is} \\ \ddot{x}_{is} + 2\xi_{is}\omega_{is}\dot{x}_{is} + \frac{f(x_{is},\dot{x}_{is},z)}{M} &= -\ddot{u}_g - \frac{\chi}{n}\mathbf{1}^T\ddot{\mathbf{x}} - \chi_T\ddot{x}_T \\ \ddot{x}_T + 2\xi_T\omega_T\dot{x}_T + \omega_T^2 x_T &= -\ddot{x}_{is} - \ddot{u}_g \end{aligned} \tag{10}$$

where $\mathbf{x}$ represents the vector of relative displacements of the superstructure, x_T and x_{is} represent TMD and isolation relative displacement respectively; u_g represents the seismic base motion; ξ and Ω are the superstructure damping and circular frequency matrices, respectively; ξ_{is} represents the viscous damping of the isolation layer and ω_{is} is the circular frequency evaluated for the rigid system oscillating on the

isolation layer having the conventional effective stiffness; ξ_T and ω_T are the tuned mass damper quantities; $M = \sum_n m_b + m_{is} + m_T$ represents the total mass of the system; χ and χ_{TMD} are the mass ratios, $\chi = \frac{\sum m_b}{M} = \frac{n \cdot m_b}{M}$, $\chi_{TMD} = \frac{m_T}{M}$; finally f/M is the hysteretic reaction of the isolator defined as BWB model (Wen 1980):

$$\frac{f(x_{is}, \dot{x}_{is}, z)}{M} = \alpha \frac{k}{M} \cdot x_{is} + (1-\alpha) \cdot \frac{k}{M} \cdot z \tag{11}$$

where the k parameter, which has a dimension of stiffness, and the non-dimensional parameter α regulate the hysteretic cycle. The above-mentioned relation can be considered as the sum of a linear term proportional to the displacement, x_{is}, and of a non-linear term in the evolving z variable, that regulates the hysteresis. This variable, which has the dimension of a displacement, is given by:

$$\dot{z} = A \cdot \dot{x}_{is} - \beta \cdot |\dot{x}_{is}| \cdot |z|^{\eta-1} \cdot z - \gamma \cdot \dot{x}_{is} \cdot |z|^{\eta} \tag{12}$$

where A, β, γ and η (Wen, 1980) represent the parameters that determine the form of the hysteretic cycle.

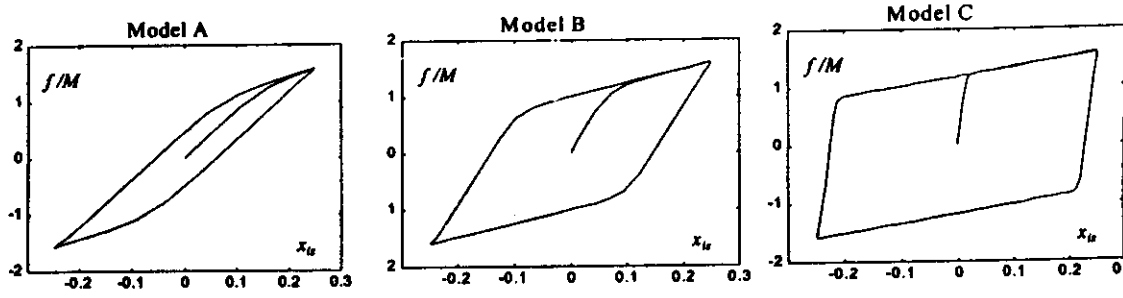

Fig. 26 Isolator types considered

This analysis considers three different types of behavior of isolator (Figure 26): low (model A), medium (model B) and high damping (model C). For each type, 5 different secant period T_{is} valued at limit displacement d_u are considered. The BWB models, which describe the behavior of such devices, are characterized by the following parameters and those of Table 1:

$$\alpha = 0.85\,;\ \beta = 0.5\,;\ \gamma = 0.5\,;\ \eta = 4$$

Table 1: BWB Adopted Parameters

		Parameter A			Parameter k/M (rad·sec^{-1})		
T_{is} [sec]	d_u [m]	Model A	Model B	Model C	Model A	Model B	Model C
T_{is}=2	0.20	15.25	37	210	4.24	3.65	2.67
T_{is}=2.5	0.25	12.4	35	300	3.2	2.75	1.89
T_{is}=3	0.30	11	38	450	2.5	2.15	1.41
T_{is}=3.5	0.35	10	40	680	1.98	1.65	1.045
T_{is}=4	0.40	8.9	47	1040	1.65	1.35	0.80

The 10-story super-structure model is characterized by the following parameters: the first four fixed base modal periods T_b = 0.67; 0.24; 0.14; 0.10 sec - damping factors ξ_b = 0.02. TMD parameters have been chosen according to optimum ones of Ioi-Ikeda (Ioi et al., 1978) for the linear system characterized by the secant period under consideration. Dynamic response is numerically carried out by the Runge-Kutta method utilizing three centered function values into the integration range.

The model response is analyzed by introducing quadratic performance indexes taking into account at the same time, both the displacement and the velocity as:

$$I_{is}(t)=\int_0^t \begin{bmatrix} x_{is} & \dot{x}_{is} \end{bmatrix} \mathbf{Q}_{is} \begin{bmatrix} x_{is} \\ \dot{x}_{is} \end{bmatrix} dt,\ I_b(t)=\int_0^t \begin{bmatrix} \mathbf{x}_b & \dot{\mathbf{x}}_b \end{bmatrix} \mathbf{Q}_b \begin{bmatrix} \mathbf{x}_b \\ \dot{\mathbf{x}}_b \end{bmatrix} dt \tag{13}$$

where the following weighting matrices are considered:

$$\mathbf{Q}_{is}=\begin{bmatrix} 1 & 0 \\ 0 & 1/\omega_{is,sec} \end{bmatrix};\ \mathbf{Q}_b=\begin{bmatrix} \mathbf{1} & \mathbf{0} \\ \mathbf{0} & 1/\omega_b \mathbf{1} \end{bmatrix}$$

The numerical analyses were carried out considering four particularly significant excitations shown in the Table 2.

Table 2: Recorded Excitations Considered in the Analysis

No.	Earthquake	Component	Duration (sec)	PGA (cm/s^2)
1	Imperial Valley (El Centro) 19/05/1940	S00E	53.80	341.82
2	Mexico City 19/09/1985	N90W	180.08	167.918
3	Montenegro (Petrovac) 1979	NS	19.62	429.29
4	Taft 21/07/1952	N69W	30.00	153.83

These seismic excitations are classified in four categories: the first is the earthquake of El Centro characterized by a strong energy content in the period interval 0.1-0.8 sec; the second category is the Petrovac earthquake with a strong energy content in the period interval 0.2-1.3 sec; the third is the Taft earthquake of low energy but having a flat response over the entire field of the period of interest; and a fourth category represented by the Mexico City earthquake which is distinguished by high peaks of acceleration response in the period interval 1.7-3 sec.

Figures 27-34 illustrate the performance index gain of the BI and TMD system compared to the BI solution, while varying the viscous damping ξ_{is} in the isolators for all the adopted isolator models. The analysis of such figures shows that the gain obtained on the base response using BI and TMD is generally positive and presents a decreasing trend when there is an increase of the viscous damping in the isolation system. The analysis also shows how the major gain is obtained for the Mexico City earthquake, which presents an elevated energetic content in the high periods of the spectra near the system resonance. Furthermore, figures show that the TMD provides benefits to the superstructure response and systems equipped with low hysteretic isolators generally present higher gain. Therefore, the presence of an elevated viscous or hysteretic damping in isolators reduces the benefit of the satellite mass damper.

Consequently, two different strategies are possible to passively control the seismic response of isolated structures: the first is based on the hysteretic or viscous dissipation at the isolation level; the second is the use of mass damping. To compare the performances of the above-mentioned strategies, Figures 35-42 show the comparison among the responses of BI with additional damping, and the one of BI and TMD. Figures show the relative gain to the two different strategies for the Mexico City and the El Centro earthquakes versus the additional damping. Results show that for the El Centro earthquake, in particular, an increase of hysteretic or viscous damping in the isolation system reduces the response of the base on one hand, but on the other noticeably worsens the response of the superstructure. Instead, the system equipped with TMD generally shows a gain on the overall system response.

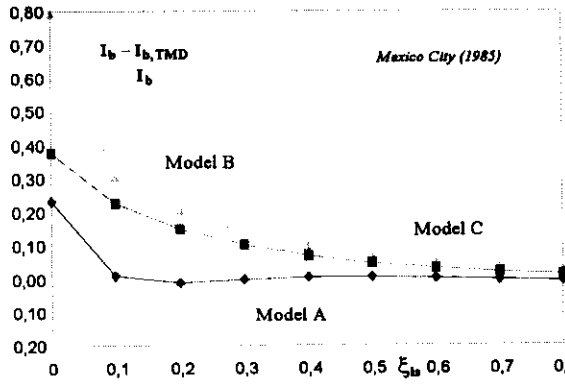

Fig. 27 Superstructure performance index gain

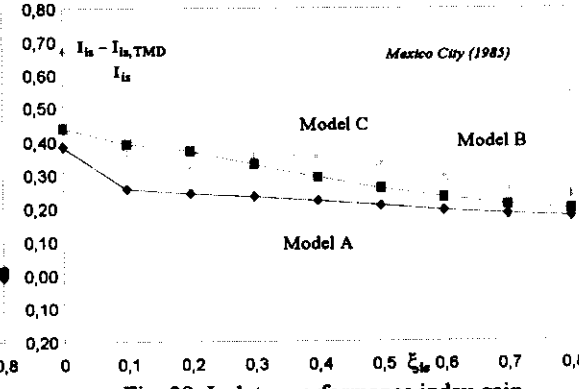

Fig. 28 Isolator performance index gain

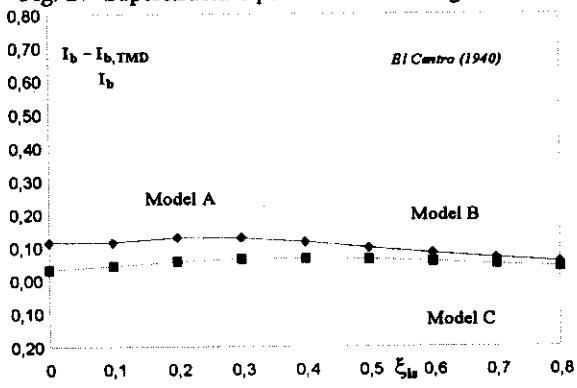

Fig. 29 Superstructure performance index gain

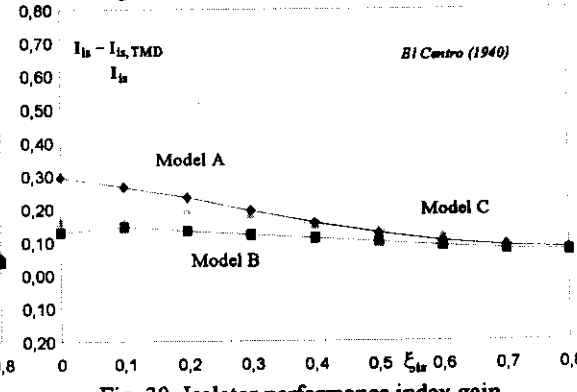

Fig. 30 Isolator performance index gain

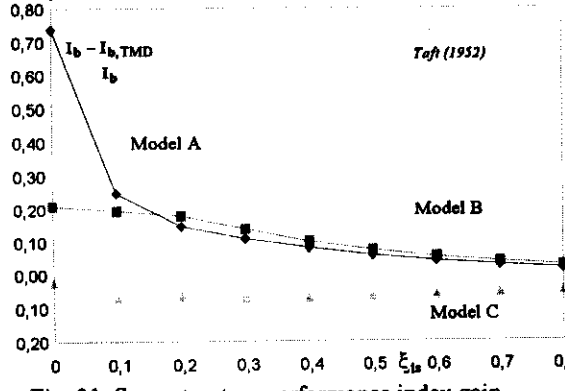

Fig. 31 Superstructure performance index gain

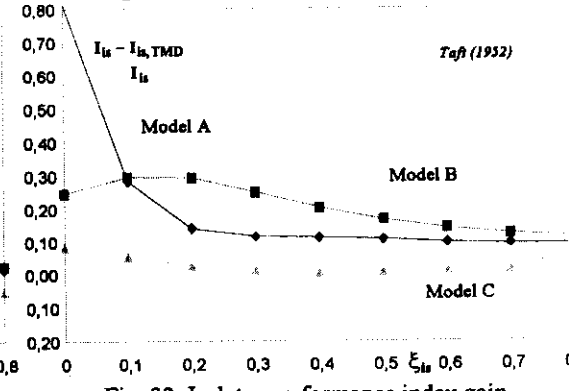

Fig. 32 Isolator performance index gain

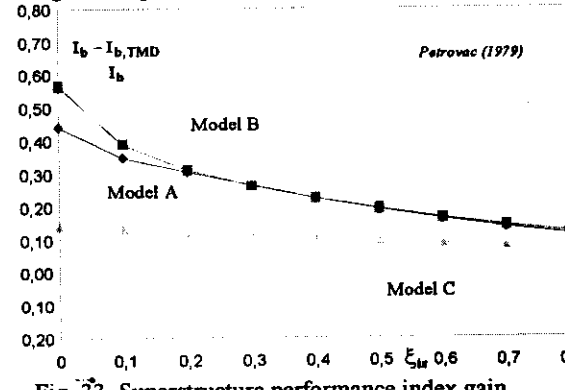

Fig. 33 Superstructure performance index gain

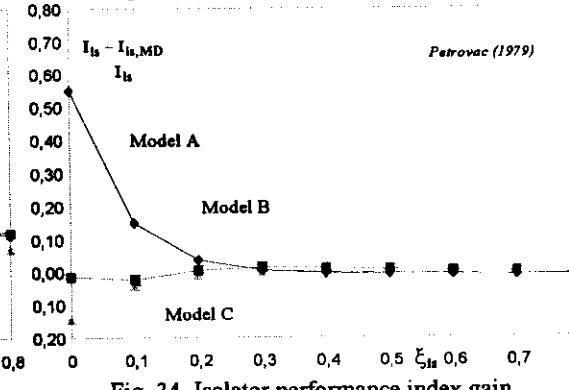

Fig. 34 Isolator performance index gain

SYSTEMS PARAMETERS
$T_b = 0.67$ sec $I_d = 3.7$ $\xi_b = 0.05$

TMD
$\chi_{TMD} = 0.1$

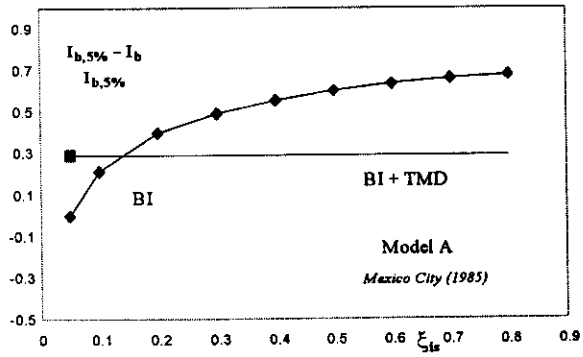

Fig. 35 Superstructure performance index gain

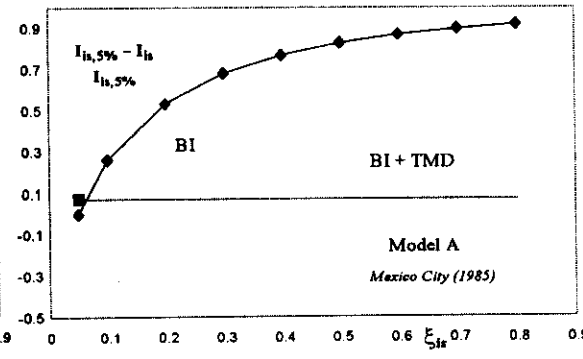

Fig. 36 Isolator performance index gain

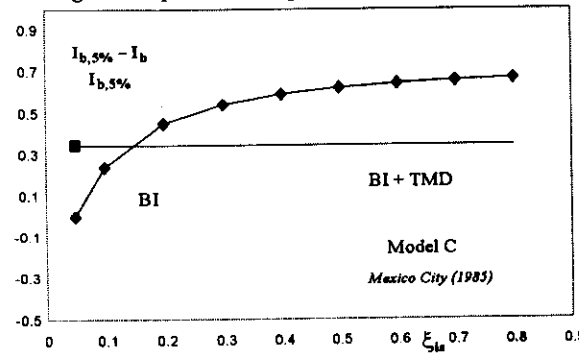

Fig. 37 Superstructure performance index gain

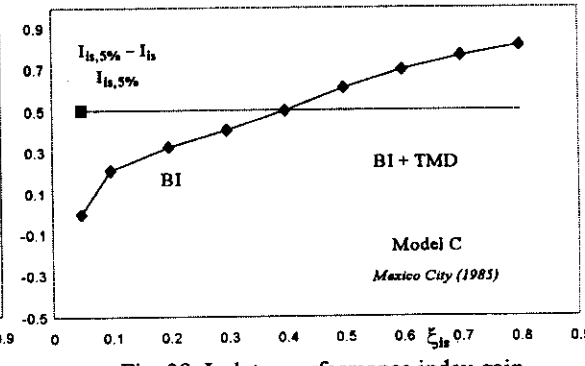

Fig. 38 Isolator performance index gain

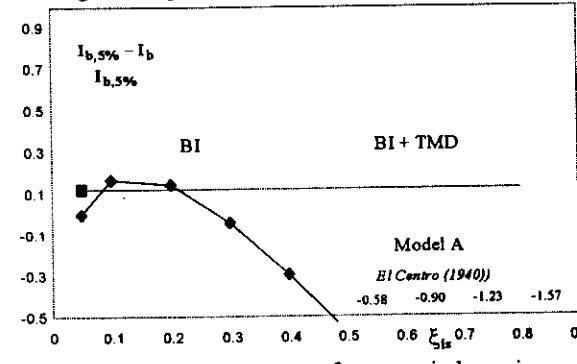

Fig. 39 Superstructure performance index gain

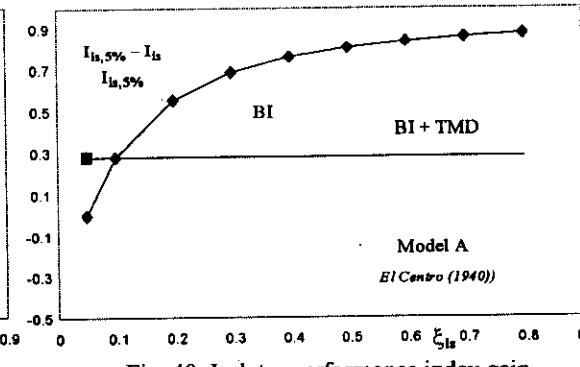

Fig. 40 Isolator performance index gain

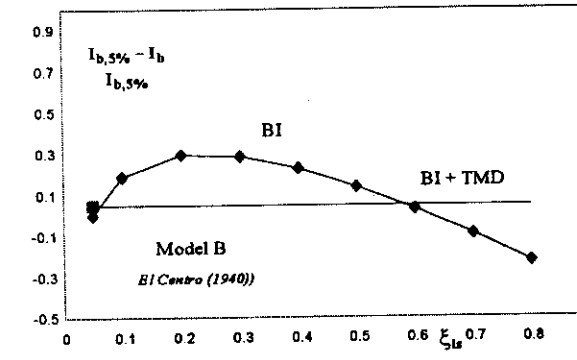

Fig. 41 Superstructure performance index gain

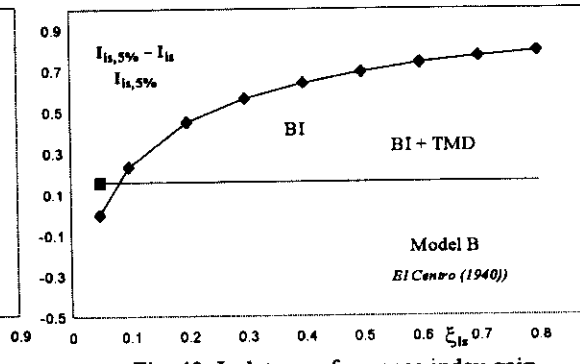

Fig. 42 Isolator performance index gain

SYSTEMS PARAMETERS
$T_b = 0.67$ sec $I_d = 3.7$ $\xi_b = 0.05$

TMD
$\chi_{TMD} = 0.1$

CONCLUSIONS

A new methodology proposed by the authors to control seismic vibrations combining base isolation (BI) with tuned mass damping (TMD) has been discussed.

The working principles of this strategy, analyzed by block diagram illustrations and by analysis in the frequency domain, have shown the specific properties which characterize this approach for reducing mechanical vibrations.

It has been shown that the dual system allows combining two filtering actions: the high frequency filtering produced by BI and the narrow frequency band reduction produced by TMD. In addition, it has been analytically demonstrated that BI primarily performs an open loop control role by acting as a superstructure input signal filter, while the TMD perform a closed loop control role.

Performance tests of the isolated systems with and without TMS have been performed through numerical simulation on linear and non-linear models subject to recorded excitations. The results presented here illustrate the potential of the new concepts for reducing vibrations.

Results in the linear range showed that the combined system offers significant gain in the seismic vibration reduction compared to the corresponding BI system which in turn, shows significant gains if compared to the fixed-base structure.

Results in the presence of isolators with non-linear behavior have determined the following:

- The use of TMD combined with BI always involves a reduction of the overall system response even in the presence of non-linear behavior of the isolators.
- Systems isolated at the base with low damping and equipped with TMD present improved performance compared to those obtained by an equivalent damping increase in the isolation.
- The introduction of TMD also improves the superstructure response while introducing supplemental dissipation in isolators often contaminates the isolation.
- The TMD efficacy decreases when there is an increase of the viscous or hysteretic damping in the isolation system, whereas it remains constant on varying the isolation degree.
- The BI and TMD combined strategy can be considered particularly efficient in reducing seismic excitations that have a strong energy content close to the resonant frequencies.

REFERENCES

1. Chang, J.C.H. and Soong, T.T. (1980). "Structural Control using Active Tuned Mass Dampers", Journal of the Engineering Mechanics Division, ASCE, Vol. 106, pp. 1091-1098.
2. Clough, R.W. and Penzien, J. (1975). "Dynamics of Structures", McGraw-Hill, New York, U.S.A.
3. Den Hartog, J.P. (1956). "Mechanical Vibrations", 4th Edition, McGraw-Hill, New York, U.S.A.
4. Frham, H. (1909). "Device for Damped Vibrations of Bodies", U.S. Patent No. 989958, Oct. 30.
5. Ioi, T. and Ikeda, K. (1978). "On the Dynamic Vibration Damped Absorber of the Vibration System", Bulletin of Japanese Society of Mechanical Engineering, Vol. 121, No. 151, pp. 64-71.
6. Kanai, K. (1957). "Semiempirical Formula for the Seismic Characteristics of the Ground", Bulletin of Earthquake Res. Inst., Univ. Tokyo, Japan, Vol. 35, pp. 309-325.
7. Kaynia, A.M., Veneziano, D. and Biggs, J.M. (1981). "Seismic Effectiveness of Tuned Mass Dampers", Journal of Struct. Div., ASCE, Vol. 107, pp. 1465-1484.
8. Kelly, J.M. (1990). "Base Isolation: Linear Theory and Design", Earthquake Spectra, Vol. 6, No. 2.
9. Kitamura, H., Fjita, T., Teramoto, T. and Kibara, H. (1988). "Design and Analysis of a Tower Structure with a Tuned Mass Damper", Proc. 9th World Conference on Earthquake Engineering, Japan, Vol. 8, pp. 415-420.
10. Ormondroy, D.J. and Den Hartog, J.P. (1928). "The Theory of the Dynamic Vibration Absorber", Trans. ASME, APM-50-7, pp. 9-22.
11. Palazzo, B. (1991). "Seismic Behaviour of Base Isolated Buildings", Proc. International Meeting on Earthquake Protection of Buildings, Ancona.

12. Palazzo, B. and Petti, L. (1994). "Seismic Response Control in Base Isolated Systems using Tuned Mass Dampers", Proceedings of the 2nd International Conference on Earthquake Resistant Construction and Design, ERCAD, Berlin, Germany, June 15-17.
13. Palazzo, B. and Petti, L. (1997). "Aspects of Structural Vibration Passive Control", Journal of MECCANICA, Vol. 32, pp. 529-544
14. Palazzo, B., Petti, L. and De Ligio, M. (1997). "Response of Base Isolated System Equipped with Tuned Mass Dampers to Random Excitations", Journal of Structural Control, Vol. 4.
15. IASMIRT (1991). "Seismic Isolation and Response Control for Nuclear and Non-nuclear structures", Special Issue for the Exhibition of the 11th International Conference on Structural Mechanics in Reactor Technology, Tokyo, Japan.
16. Villaverde, R. (1994). "Seismic Control of Structure with Damped Resonant Appendages", Proc. First World Conference on Structural. Control, Vol. 1, WP4-113-WP4-122.
17. Tajimi, H. (1960). "A Statistical Method of Determining the Maximum Response of a Building Structure during an Earthquake", Proc. 2nd World Conf. on Earthq. Eng., Japan, pp. 781-797.
18. Wen, Y.K. (1980). Journal of Applied Mechanics, Vol. 47, p. 50